Selective agonists and antagonists of α9 versus α7 nicotinic acetylcholine receptors

Roger L. Papke[1]*, Hina Andleeb[2], Clare Stokes[1], Marta Quadri[2], and Nicole A. Horenstein[2]

[1]Department of Pharmacology and Therapeutics, University of Florida, PO Box 100267 Gainesville, FL 32610 USA (CS, RLP)

[2]Department of Chemistry, University of Florida, PO Box 117200, Gainesville, FL 32611-7200 USA (HA, MQ, NAH)

*To whom correspondence should be addressed:

Roger L. Papke, Ph.D.

rlpapke@ufl.edu

Department of Pharmacology and Therapeutics

University of Florida, PO Box 100267

Gainesville FL, 32610-0267

In Press: ACS: Neuroscience

α9 agonists and antagonists

Abstract

Nicotinic acetylcholine receptors containing α9 subunits are essential for auditory function and have been implicated, along with α7-containing nicotinic receptors, as potential targets for the treatment of inflammatory and neuropathic pain. The study of α9-containing receptors has been hampered by the lack of selective agonists. The only α9-selective antagonists previously identified are peptide conotoxins. Curiously, the activity of α7 and α9 receptors as modulators of inflammatory pain appears to not rely strictly on ion channel activation, which led to the identification of α7 "silent agonists" and phosphocholine as an "unconventional agonist" for α9 containing receptors. The parallel testing of the α7 silent agonist *p*-CF_3-diEPP and phosphocholine led to the discovery that *p*-CF_3-diEPP was an α9 agonist. In this report, we compared the activity of α7 and α9 with a family of structurally-related compounds, most of which were previously shown to be α7 partial or silent agonists. We identify several potent α9-selective agonists as well as numerous potent and selective α9 antagonists and describe the structural basis for these activities. Several of these compounds have previously been shown to be effective in animal models of inflammatory pain, activity that was assumed to be due to α7 silent agonism but may, in fact, be due to α9 activity. The α9-selective conotoxin antagonists have also been shown reduce pain in similar models. Our identification of these new α9 agonists and antagonists may prove to be invaluable for defining an optimal approach for treating pain, allowing for reduced use of opioid drugs.

Keywords: nicotinic, pharmacology, voltage clamp, drug development, hearing, inflammation,

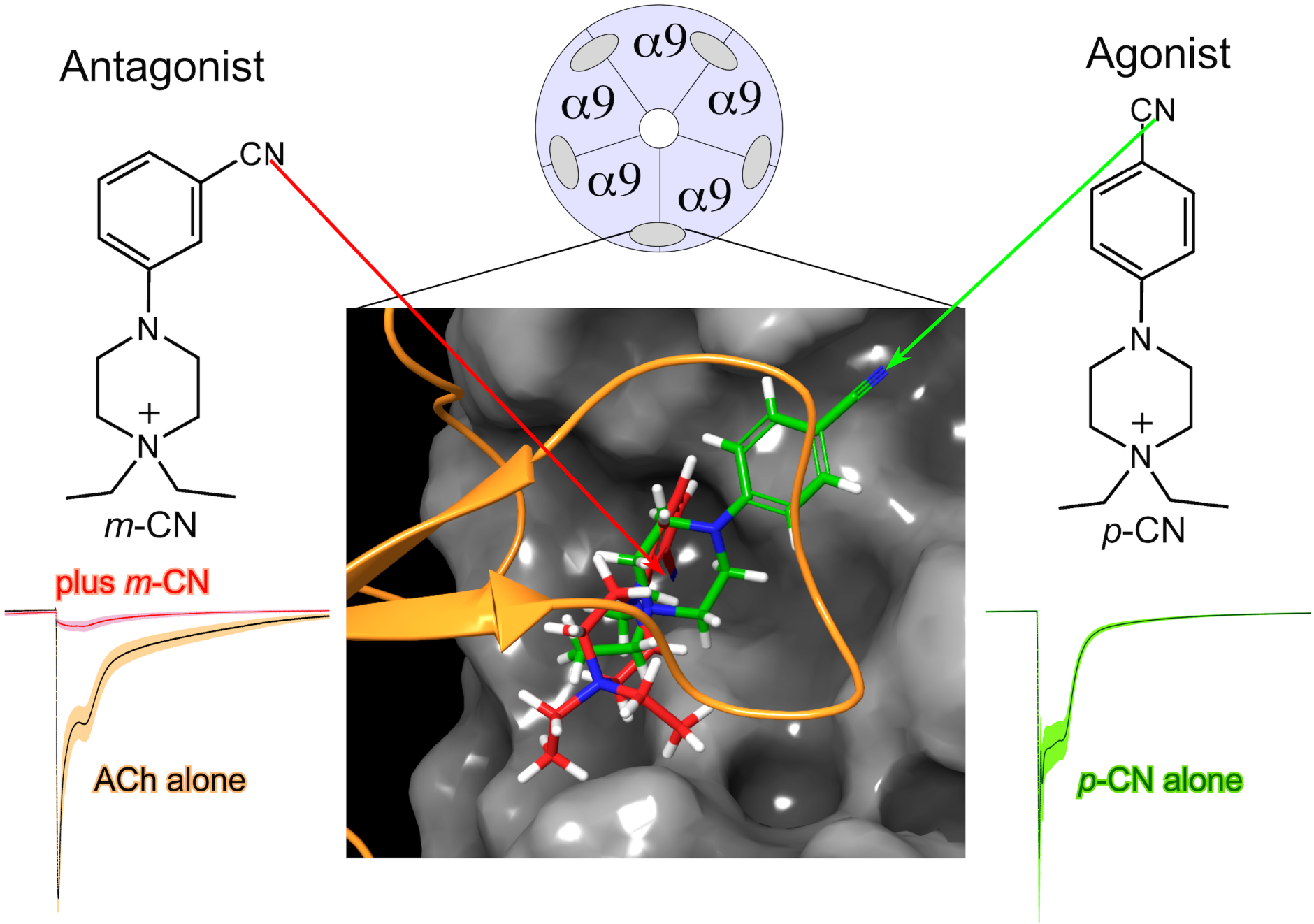
Antagonist
α9
α9
α9
α9
α9
Agonist
CN
N
+
N
m-CN
CN
N
+
N
p-CN
plus m-CN
ACh alone
p-CN alone

α9 agonists and antagonists

Introduction

Nicotinic acetylcholine receptors (nAChR) have long been known to mediate effects of the neurotransmitter acetylcholine in the central and peripheral nervous systems, and by the late 1980s the genes coding for most of the nAChR subunits had been cloned [1]. In the early 1990s, members of the Heinemann lab at the Salk Institute took up the challenge to solve one of the last mysteries in nicotinic cholinergic function, the molecular basis for the modulation of auditory function by efferent cholinergic innervation to the inner ear. Early anatomical studies [2] had identified cholinergic efferent fibers innervating outer hair cells of the cochlea that were postsynaptic to brainstem neurons projecting from the superior olivary complex. Activation of these fibers could suppress afferent output from the cochlea with atypical cholinergic pharmacology [3] and was sensitive to block by α-bungarotoxin (α-BTX) [4].

In 1994 Belen Elgoyhen and colleagues reported the isolation of α9, cloned from a rat olfactory epithelium cDNA library [5]. Although, compared to other nAChR clones, the original α9 clone did not express very well in *Xenopus* oocytes, the gene formed functional homomeric α-BTX-sensitive receptors with unique mixed pharmacological properties, insensitive to nicotine but sensitive to some muscarinic ligands [6]. Knockout of the α9 gene resulted in the loss of auditory function [7]. A related gene, α10, was subsequently cloned [8-9], and data suggest that the primary receptors of the inner ear are pentameric combinations of α9 and α10 subunits with a likely stoichiometry of two α9 and three α10 subunits [10]. These receptors can generate outward currents in hair cells due to ability of calcium influx through the receptors to activate calcium-dependent (SK2-containing) potassium channels [11].

While a single report suggested the α9α10 receptors were expressed in mouse brain [12], most studies indicate that these receptors are not found in adult brain [13]. However, although these receptors are essential for auditory function, their expression is by no means restricted to the inner ear. Expression of α9α10 has been described in dorsal root ganglion neurons [14-15], lymphocytes, skin keratinocytes, the pars tuberalis of the pituitary [16], and alveolar macrophages, as well as in the lung parenchyma of native and transplanted lungs [17]. Although the presence of both α9α10 RNA and protein has been confirmed in various non-neuronal cells, evidence is lacking that they form functional ion channel receptors in these tissues [18]. However, the expression of α9α10 in these tissues, especially cells of the immune system, supports a role for these receptors in the cholinergic anti-inflammatory pathway (CAP) [19]. Natural activation of CAP is believed to be mediated by ACh released into the blood by the vagus nerve [20], and pharmacological targeting of the system was first observed with selective agonists for α7 nAChR [21] and often with agonists that had low efficacy for channel activation [22-23], suggesting that α7 receptors in immune cells mediate metabotropic rather than ionotropic signaling [24]. There are both interesting parallels and differences in the apparent roles of α9 and α7 nAChR in CAP, brought to light largely by the identification of conotoxins, including ArIB [25] and RgIA4 [26], that are selective antagonists for either α7 or α9α10 receptors, respectively. While the down-regulation of inflammatory cytokines mediated by α7 receptors is associated with α7 agonists, albeit ones with low ion channel efficacy [22, 27], the putative CAP-mediated reduction of inflammation by α9 has primarily been associated with antagonists, usually toxins like RgIA4 [28-29].

α9 agonists and antagonists

Interestingly, an alternative hypothesis has been generated based on the identification of phosphocholine as an unconventional agonist for α9 receptors, able to selectively activate metabotropic functions of α9 [30]. Recently, phosphocholine and the putative α7 silent agonist *p*CF_3-diEPP [31] were compared for their ability to modulate pro-inflammatory cytokine release by human peripheral blood mononuclear leukocytes, monocytic THP1-cells, and THP-1-derived M1-like macrophages. Both agents were found to be effective, and based on sensitivity to α7 and α9-selective conotoxins, required activation of both α7 and α9 nAChR (Richter *et al.*, in press). While, at the very least, these results would seem to contradict the hypothesis that CAP is regulated in opposite ways by α7 and α9 receptors, they also brought to light the fact that *p*CF_3-diEPP, previously believed to be α7 selective, was in fact a relatively efficacious α9 agonist.

pCF_3-diEPP was one of a series of 1,1-diethyl-4-phenylpiperazin-1-ium derivatives previously characterized for their activity on α7 as weak partial or silent agonists [32]. Identification of the α9 agonist activity of *p*CF_3-diEPP led us to re-evaluate the entire family of compounds. We found some that were potent α9-selective agonists while others were potent α9 antagonists. Comparing and contrasting these compounds in the context of a structural model for α9 permitted us hypothesize the basis for these differing activities and generate new compounds to confirm these hypotheses. Our results greatly enlarge the scope of pharmacological agents available for the investigation of α9 nAChR functions, and encourage re-evaluation of previous studies assumed to depend on α7 silent agonism.

Results and discussion

Test compounds

We conducted our initial screen for α9 active compounds with a family of 27 compounds previously tested for their activity on α7 receptors (Table 1). The compounds utilized six different structural scaffolds (Figure 1). The majority of the compounds (21/27) were based on the diEPP (1,1-diethyl-4-phenylpiperazin-1-ium) scaffold. The α7 activity of these compounds, along with those based on scaffolds 2, 3, and 4, were previously published [32]. Compounds ranged from partial agonists with up to 35% the efficacy of ACh, to silent agonists which only activated the receptor when co-applied with a strong positive allosteric modulator such as PNU-120596. The α7 activity of the sulfonium analog of the diEPP compounds, EPTMO (scaffold 6), was also previously published [33]. The two compounds with a cyclic rather than diethyl base structure (scaffold 5) have not previously been published.

α9 agonists and antagonists

Table 1 test compounds

Scaffold 1: diEPP

Short name	R_1	R_2	R_3	IUPAC name
diEPP	H	H	H	1,1-diethyl-4-phenylpiperazin-1-ium
o-meth	H	H	CH_3	1,1-diethyl-4-(o-tolyl)piperazin-1-ium
m-OH	H	OH	H	1,1-diethyl-4-(3-hydroxyphenyl)piperazin-1-ium
p-Br	Br	H	H	4-(4-bromophenyl)-1,1-diethylpiperazin-1-ium
p-CN	CN	H	H	4-(4-cyanophenyl)-1,1-diethylpiperazin-1-ium
p-Cl CL	H	H4-(4-chlorophenyl)-1,1-diethylpiperazin-1-ium		
p-CONH	$CONH_2$	H	H	4-(4-carbamoylphenyl)-1,1-diethylpiperazin-1-ium
p-MeO	OCH_3	H	H	1,1-diethyl-4-(4-methoxyphenyl)piperazin-1-ium
m-F	H	F	H	1,1-diethyl-4-(3-fluorophenyl)piperazin-1-ium
m-CONH	H	$CONH_2$	H	4-(3-carbamoylphenyl)-1,1-diethylpiperazin-1-ium
m-Br	H	Br	H	4-(3-bromophenyl)-1,1-diethylpiperazin-1-ium
p-CF_3	CF_3	H	H	1,1-diethyl-4-(4-(trifluoromethyl)phenyl)piperazin-1-ium
m-CN	H	CN	H	4-(3-cyanophenyl)-1,1-diethylpiperazin-1-ium
m-Cl	H	Cl	H	4-(3-chlorophenyl)-1,1-diethylpiperazin-1-ium
diMeO	OCH_3	H	OCH_3	4-(2,4-dimethoxyphenyl)-1,1-diethylpiperazin-1-ium
p-meth	CH_3	H	H	1,1-diethyl-4-(p-tolyl)piperazin-1-ium
p-Fl F	H	H1,1-diethyl-4-(4-fluorophenyl)piperazin-1-ium		
m-CF_3	H	CF_3	H	1,1-diethyl-4-(3-(trifluoromethyl)phenyl)piperazin-1-ium
m-meth	H	CH_3	H	1,1-diethyl-4-(m-tolyl)piperazin-1-ium
m-MeO	H	OCH_3	H	1,1-diethyl-4-(3-methoxyphenyl)piperazin-1-ium

Scaffold 2

BdPip — 4-benzylidene-1,1-diethylpiperidin-1-ium

Scaffold 3

DIPPA — 1,1-diethyl-4-(phenylamino)-1λ^4-piperidin-2-ylium

Scaffold 4:

2-nap — 1,1-diethyl-4-(naphthalen-2-yl)piperazin-1-ium

Scaffold 5

PhDu — 3-phenyl-3,6-diazaspiro[5.5]undecan-6-ium

CF_3PhDu — 3-(4-(trifluoromethyl)phenyl)-3,6-diazaspiro[5.5]undecan-6-ium

Scaffold 6

EPTMO — 1-ethyl-4-phenylthiomorpholin-1-ium

α9 agonists and antagonists

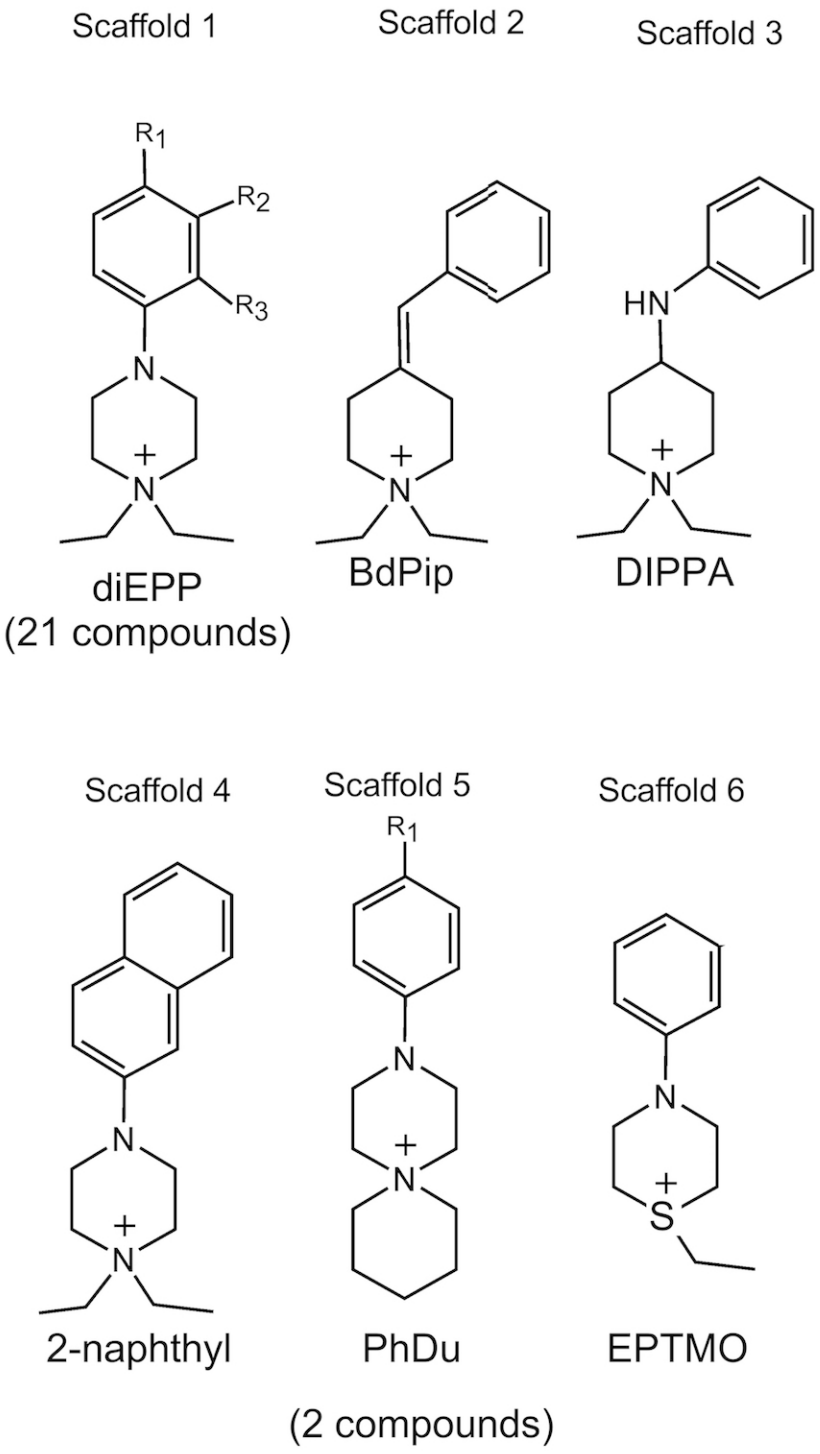

Figure 1. Structural scaffolds of test compounds. The test compounds (Table 1) were based on the diEPP scaffold or derivatives thereof.

Initial screens on α7 and α9 nAChR

Test compounds were applied to oocytes co-expressing α9 and rapsyn, at 100 μM alone or co-applied with 60 μM ACh, and the results compared to those previously obtained with α7 receptors

α9 agonists and antagonists

(Figures 2-3). For clarity of presentation, the compounds using the diEPP scaffold are ordered based on the size of the α7 responses when applied alone at 30 μM. With the exception of *p*-CN-diEPP (p-CN), the five most efficacious α7 partial agonists (Figure 2 upper group) produced little or no activation of α9 receptors. *p*-CN appeared to be a full agonist of α9 and as such did not inhibit ACh-evoked responses when co-applied. In contrast, all of the other compounds in this diEPP group not only failed to activate α9 receptors but effectively suppressed the ACh-evoked response when co-applied. Among the second group of α7 partial agonists (Figure 2 lower tier), *p*-CONH and *p*-CF_3 stood out as α9 agonists, while all the rest were α9 antagonists.

In the third and fourth groups, which were compounds that also had little or no α7 efficacy when applied alone (Figure 3), the compounds were all α9 antagonists at the concentration tested, substantially reducing α9 ACh-evoked responses when co-applied at 100 μM. In these groups, only *p*-F qualified as an α7 silent agonist.

With the exception of DIPPA, the compounds based on the alternative scaffolds tended to be α7 partial agonists (Figure 4). Several of the compounds in this group were α9 agonists, the most active ones being the two on the PhDu scaffold.

α9 agonists and antagonists

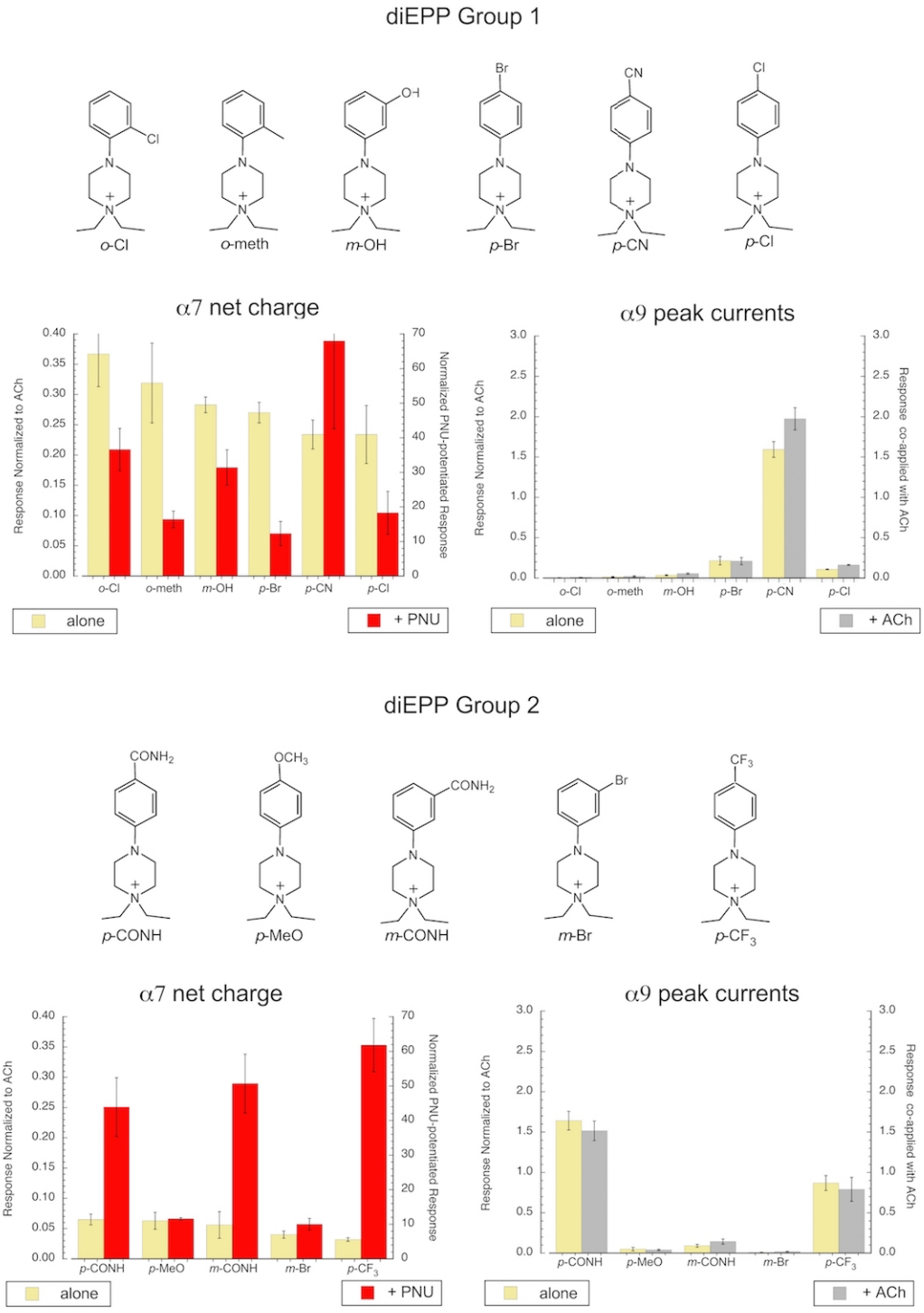

Figure 2. Activity of α7 partial agonists based on the diEPP scaffold. Plots on the left show the effects on the test compounds applied at 30 μM to cells expressing α7. Yellow bars (left axis) reflect the net-charge response relative to 60 μM ACh controls when the compounds were applied alone. Gray bars (right axis) show the net-charge responses when the compounds were co-applied with10 μM of the PAM PNU-120596. Plots on the right show the activation (peak currents) of cells expressing α9 to the application of the test compounds applied alone at 100 μM, relative to the average of two control applications of 60 μM ACh (yellow bars, left axis), and the ability of the test compounds co-applied at 100 μM to inhibit the 60 μM ACh-evoked responses (gray bars, right axis). All bars represent the averages of 5-8 cells (± SEM).

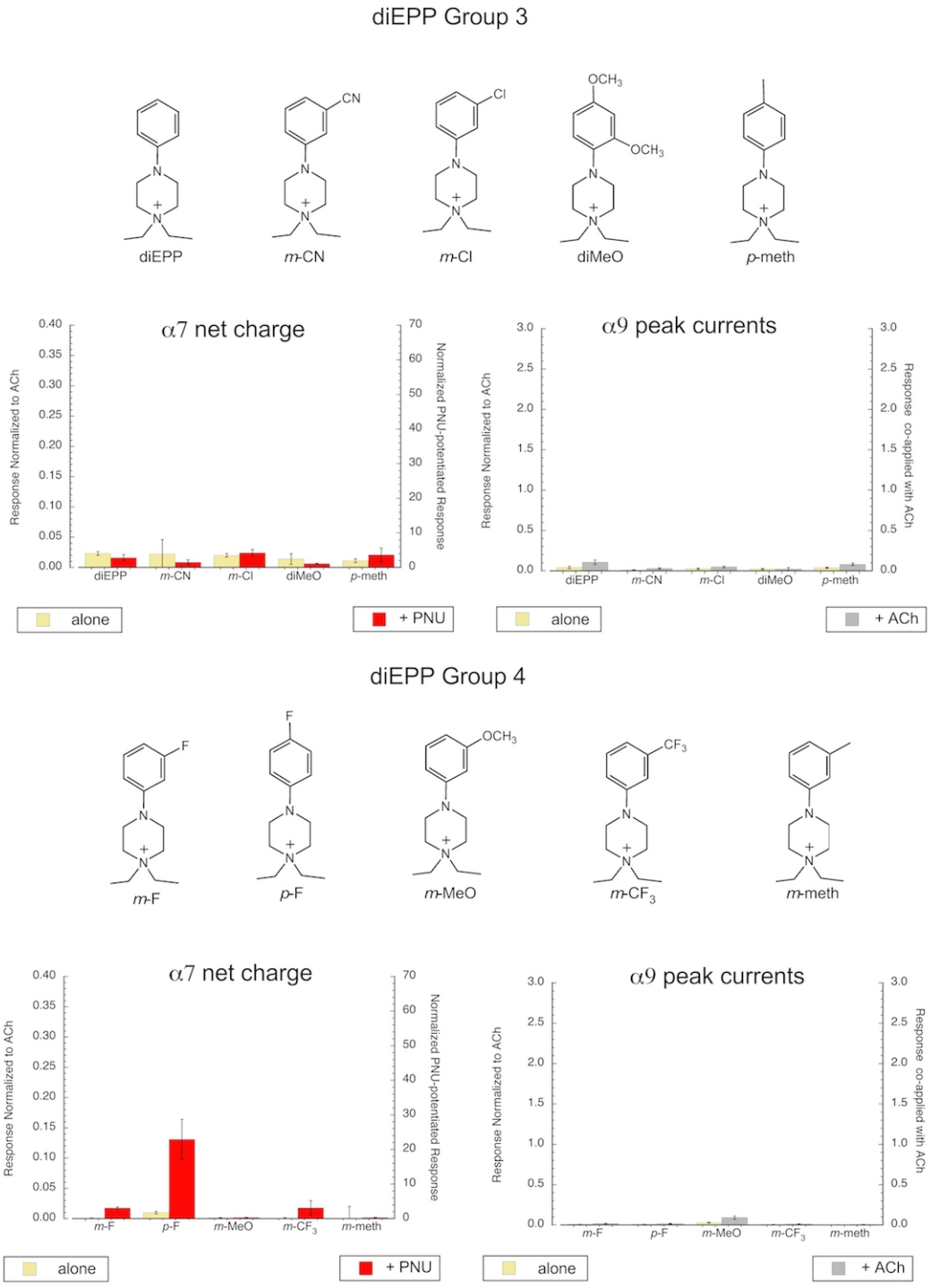

Figure 3. Activity of test compounds on the diEPP scaffold with little or no efficacy for α7 activation. Plots on the left show the effects on the test compounds applied at 30 μM to cells expressing α7. Yellow bars (left axis) reflect the net-charge response relative to 60 μM ACh controls when the compounds were applied alone. Gray bars (right axis) show the net-charge responses when the compounds were co-applied with10 μM of the PAM PNU-120596. Plots on the right show the activation (peak currents) of cells expressing α9 to the application of the test compounds applied alone at 100 μM, relative to the average of two control applications of 60 μM ACh (yellow bars, left axis), and the ability of the test compounds co-applied at 100 μM to inhibit the 60 μM ACh-evoked responses (gray bars, right axis). All bars represent the averages of 5-8 cells (± SEM).

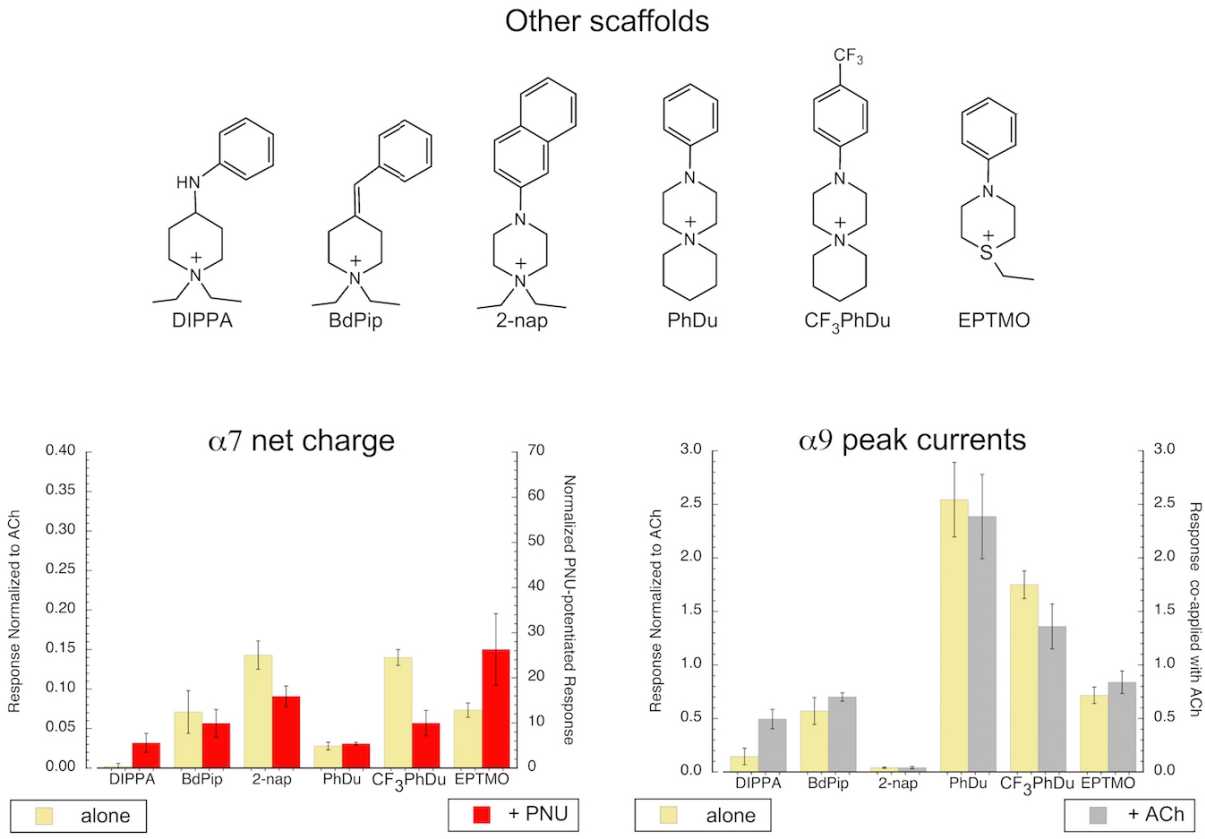

Figure 4. Activity of test compounds with alternative structural scaffolds. Plots on the left show the effects on the test compounds applied at 30 μM to cells expressing α7. Yellow bars (left axis) reflect the net-charge response relative to 60 μM ACh controls when the compounds were applied alone. Gray bars (right axis) show the net-charge responses when the compounds were co-applied with10 μM of the PAM PNU-120596. Plots on the right show the activation (peak currents) of cells expressing α9 to the application of the test compounds applied alone at 100 μM, relative to the average of two control applications of 60 μM ACh (yellow bars, left axis), and the ability of the test compounds co-applied at 100 μM to inhibit the 60 μM ACh-evoked responses (gray bars, right axis). All bars represent the averages of 5-8 cells (± SEM).

Characterization of α9 agonists

Based on the preliminary screens, we selected five compounds that were the most effective activators of α9 for further characterization. These included the two compounds on the PhDu scaffold and three of diEPP analogs with substitutions in the para position. Two other diEPP analogs with substitutions in the para position, *p*-Br and *p*-Cl showed small α9 responses and partial antagonism of α9 ACh-evoked responses, and we also choose to investigate these dual activities with *p*-Br-diEPP. The compounds varied in potency and efficacy (Figure 5, Table 2) with several being more potent than ACh and at least as efficacious. *p*-CF_3 was a partial agonist with intermediate efficacy and *p*-Br was a low efficacy partial agonist.

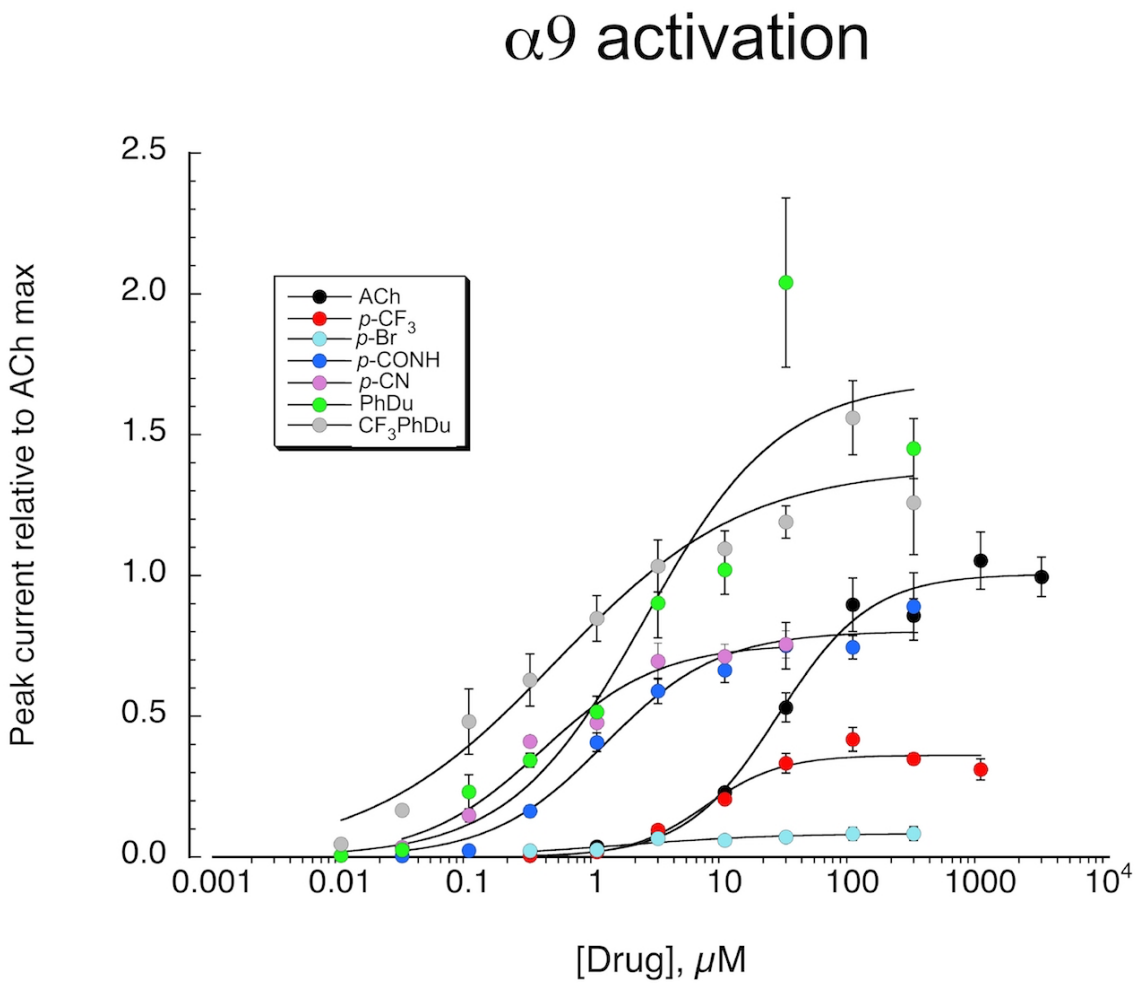

Figure 5. Concentration-response relationships of test compounds for the activation of cells expressing α9 compared to ACh responses. Data represent the average peak-current responses of 5-8 cells (± SEM) at each concentration. The test compound applications were alternated with control applications of 60 μM ACh to confirm the stability of the control ACh responses. Experiment responses were measured relative to the preceding ACh control responses and then normalized relative to the ratio of the ACh controls to the ACh maximum (0.63). The Levenberg–Marquardt algorithm was used to fit a Hill equation to the data using (Kaleidagraph 4.5.2). Fit parameters and statistics are provided in Table 2.

Table 2.
α9 activation

	EC_{50}, μM	n*	I_{Max}	ChiSq	R
ACh	26 ± 4	1.2 ± 0.2	1.00 ± 0.04	0.018	0.994
p-CF_3	7.04 ± 1.88	1.5 ± 0.5	0.36 ±0.02	0.007	0.974
p-Br	1.55 ±0.90	0.7 ± 0.3	0.084 ± 0.01	0.0004	0.948
p-CONH	1.15 ± 0.25	1.0 ± 0.2	0.80 ±0.04	0.0173	0.990
p-CN	0.368 ± 0.10	0.9 ± 0.2	0.76 ± 0.05	0.0118	0.988
PhDu	2.38 ± 1.52	0.8 ± 0.3	1.69 ± 0.22	0.4325	0.950
CF_3PhDu	0.475 ± 0.22	0.9 ± 0.1	1.38 ± 0.10	0.0976	0.977

α9 agonists and antagonists

*The values "n" are the Hill coefficients of the fits. It should be noted however that in these functional studies that convolute simultaneous activation and desensitization with the kinetics of solution exchange there is no straightforward interpretation of these values.

Characterization of α9 antagonists

The profiles of nineteen of the original compounds screened (Figures 2-4) were consistent with α9 antagonism and we initially chose a set of five compounds for detailed characterization (Figure 6A). Of the compounds based on the diEPP scaffold, o-Cl was selected for this first group because it was the most efficacious α7 partial agonist. As noted above, the active α9 agonists on the diEPP scaffold all had a substitution in the para position, so we choose to characterize two putative antagonists that also had para substitutions, *p*-F and *p*-Cl. The diEPP compounds with CN and CF_3 groups in the para position were efficacious agonists, so we choose the diEPP compounds with the same substitutions in the meta position for further characterization as antagonists.

The compounds were co-applied with 60 mM ACh, and the results (Figure 6A) indicated that most of the compounds, with the exception of *m*-CN, were effective antagonists at concentrations less than 10 μM (Table 3). However, *p*-Br had a low level of α9 agonist activity, which limited its antagonism of ACh evoked responses.

Of the remaining candidate antagonists, we further tested the nine compounds that gave the greatest antagonism of α9 when co-applied at 100 μM. We initially evaluated their antagonist activity when co-applied with ACh at a concentration of 3 μM (Figure 6B). Of these, we selected four compounds that gave greater than 75 % inhibition at 3 μM for further testing (Figure 6C). Three of these compounds; *p*-Meo, 2-Nap, and diMeO, had IC_{50}s of less than one μM (Table 3).

In order to evaluate the mechanism of α9 antagonism by diEPP compounds, we conducted a competition experiment to determine if inhibition of ACh responses by one representative compound, *p*-F, could be overcome by application of ACh at higher concentrations (Figure 6D). When ACh was co-applied with 5 μM *p*-F, approximately the IC_{50} concentration (Table 3), the ACh EC_{50} was increased from 26 ± 4.2 μM to 333 ± 14 μM with no decrease in the I_{Max}. This indicates that the diEPP antagonists are competing with ACh for the same binding sites on the α9 receptor. This is reasonable since all of the diEPP compounds have a core structure corresponding to DMPP (Dimethylphenylpiperazinium), a classic agonist of ganglionic receptors.

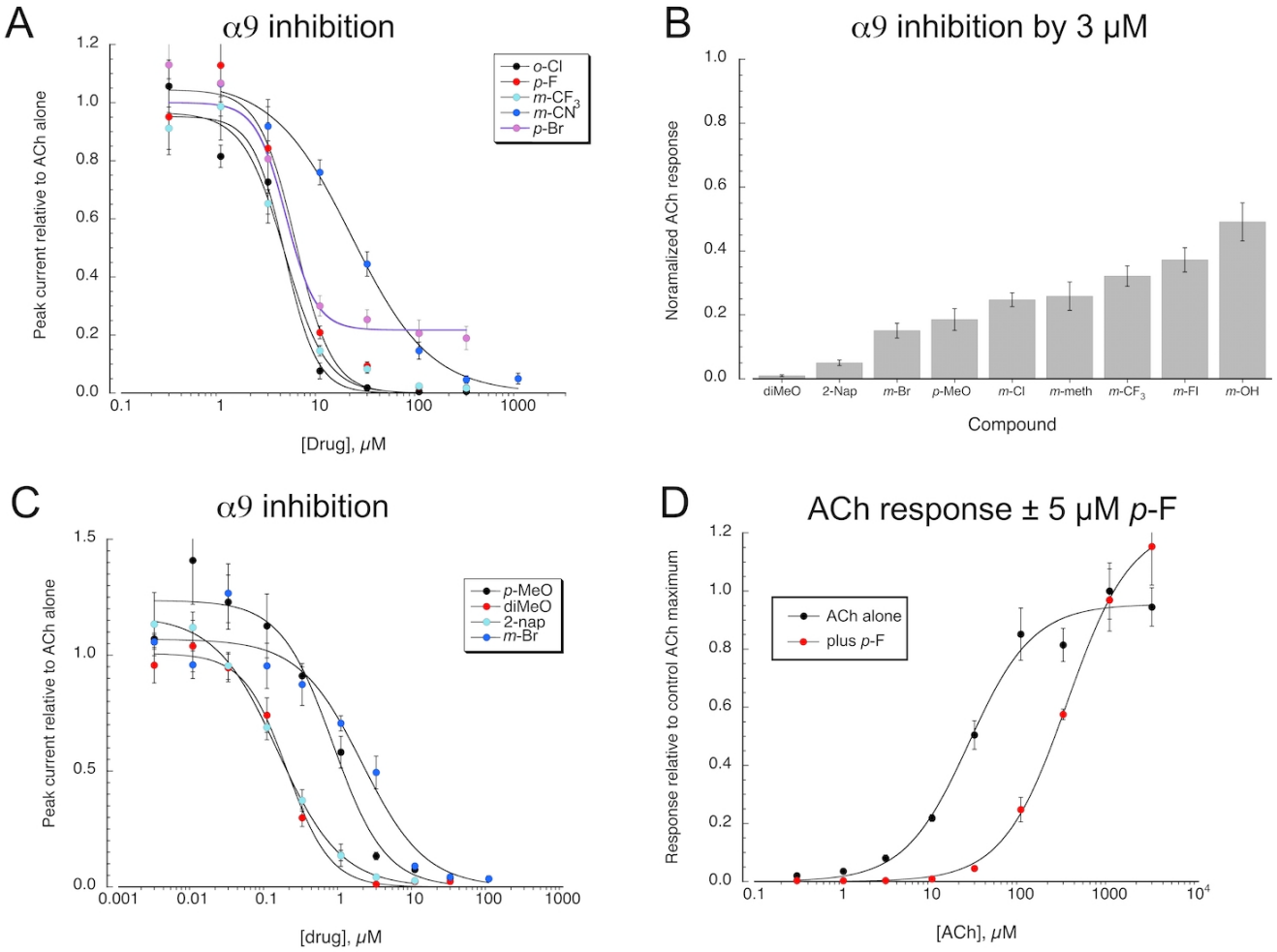

Figure 6. Inhibition of α9 ACh-evoked responses. **A)** Concentration-response relationships of initially selected test compounds for the inhibition the ACh responses of cells expressing α9. Experiment responses were measured relative to the preceding ACh control response. Fit parameters and statistics are provided in Table 2. **B)** Further screen at 3 μM of compounds that gave greater than 90% inhibition of ACh when co-applied with ACh at 100 μM. Data represent the average peak-current responses of 7-8 cells (± SEM). The four most active compounds were selected for further analyses. **C)** Concentration-response relationships of the four most active compounds identified in panel B for the inhibition the ACh responses of cells expressing α9. Data in A and C represent the average peak-current responses of 5-8 cells (± SEM) at each concentration. The test compound applications were alternated with control applications of 60 μM ACh to confirm the stability of the control ACh responses. Experiment responses were measured relative to the preceding ACh control response. The Levenberg–Marquardt algorithm was to fit the Hill equation assuming a negative Hill slope to the data in A and C using (Kaleidagraph 4.5.2). Fit parameters and statistics are provided in Table 3. D) Mechanism of α9 inhibition by *p*-F. Peak current responses to ACh (see also Figure 7) were compared to the responses obtained when ACh was co-applied with 5 μM *p*-F.

α9 agonists and antagonists

Table 3. α9 inhibition

	IC_{50}, μM	n	ChiSq	R
o-Cl	4.45 ± 0.77	-2.7 ± 0.9	0.026	0.989
p-F	5.67 ± 0.96	-2.4 ± 0.6	0.025	0.991
m-CF_3	4.42 ± 0.56	-2.1 ± 0.4	0.012	0.995
m-CN	21 ± 2.71	-1.1 ± 0.1	0.005	0.998
p-Br*	4.56 ± 0.98	-2.8 ±1.1	0.025	0.988
p-MeO	0.78 ± 0.19	-1.2 ± 0.31	0.069	0.9848
m-Br	1.93 ± 0.59	1.0 ± 0.3	0.077	0.979
2-Nap	0.14 ±0.007	-1.0 ± 0.04	0.001	0.997
diMeO	0.188 ± 0.020	-1.5 ± 0.2	0.010	0.997

*Inhibition by *p*-Br only to 0.217 ± 0.05

Co-expression of α9 and α10

In vivo, α9 often co-assembled with α10, and we investigated whether the co-expression of α10 affected the basic activity of our test compounds. The ACh responses of cells expressing α9α10 are typically somewhat larger than those expressing α9 alone. The kinetics of the 60 μM ACh-evoked responses are also somewhat different but not very much so (Figure 7A inserts). For α9 expressed alone, the EC_{50} for peak currents and net charge were 26 ± 4 μM and 99 ± 33 μM, respectively. For α9 co-expressed with α10, the EC_{50} for peak currents and net charge were 30 ± 10 μM and 69 ± 19, respectively (Figure 7A). We compared the 100 μM responses of several key compounds and found no significant differences between α9 and α9α10 (Figure 9B), except for p-Br, which evoked small responses from α9 and even smaller responses from α9α10 ($p < 0.05$ after correction for multiple comparisons).

We evaluated p-CF_3, a partial agonist for α9 (Figure 6) with an EC_{50} of 7.04 ± 1.88 μM and an I_{Max} of 0.36 ±0.02 (Table 2), and confirmed that it is likewise a partial agonist for α9α10 receptors with an EC_{50} of 6.5 ± 1.88 μM and an I_{Max} of 0.27 ±0.01 (Figure 7C). We tested three of the α9 antagonists and determined that they were also antagonists of α9α10, with similar potencies. The IC_{50} values for *o*-Cl, *p*-F, and *m*-CF3 were 1.56 ± 0.07 μM, 8.8 ± 3.8 μM, and 4.07 ± 1.6 μM, respectively (compare to Table 2).

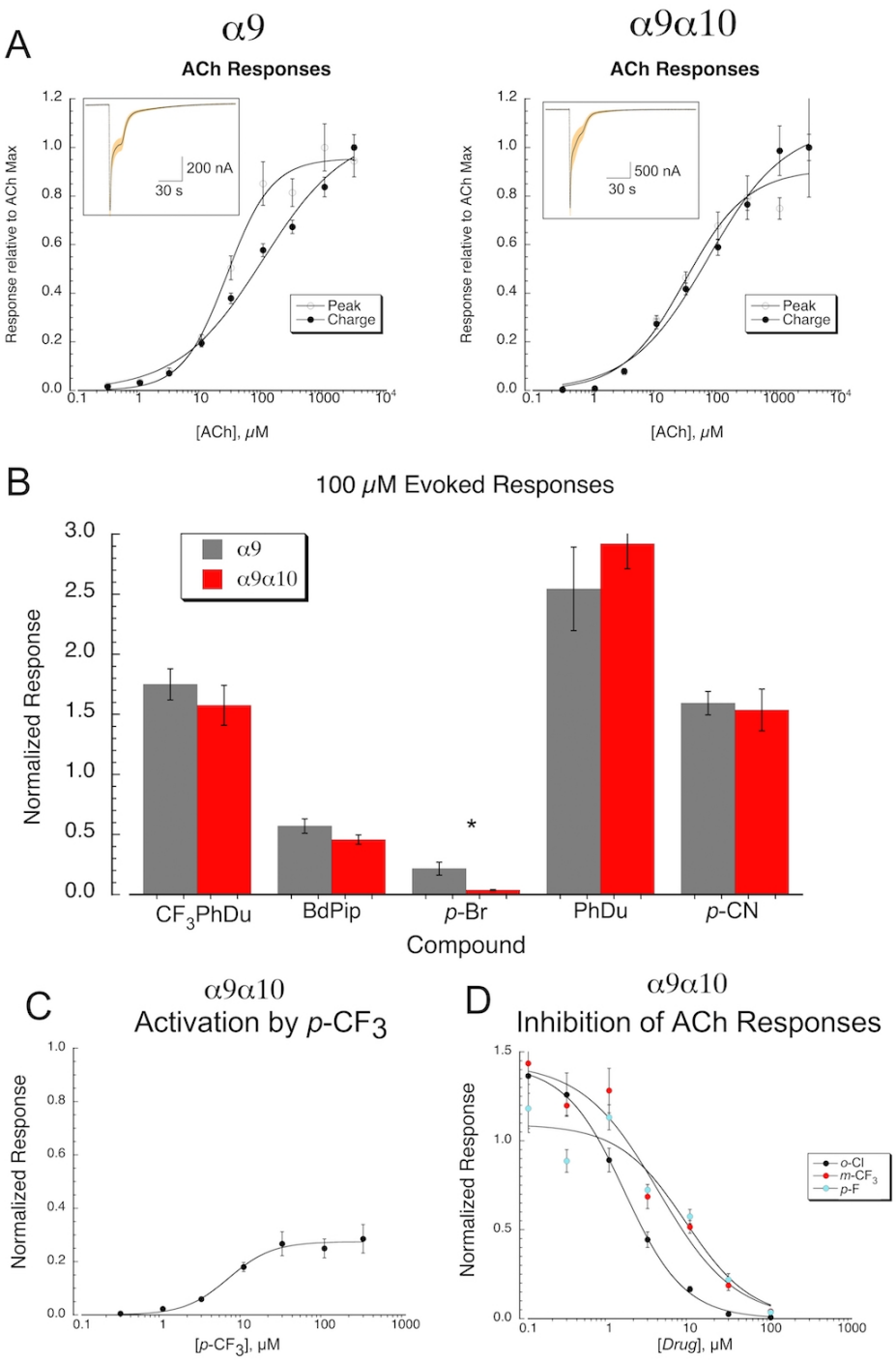

Figure 7. Impact of α10 co-expression. **A)** ACh responses of cells expressing α9 alone or co-expressed with α10. Data represent the average peak-current responses (± SEM, n = 7 for α9 and n = 6 for α9α10) over a range of ACh concentrations. Applications of increasing ACh concentrations were alternated with control applications of 60 μM ACh to confirm the stability of the control ACh responses. Experimental responses were measured relative to the preceding ACh control responses and then normalized relative to the ratio of the ACh controls to the ACh maximum (0.63 for α9 and 0.60 for α9α10). Data were calculated for both peak currents and net-charge responses. The inserts show the average control ACh response. **B)** Averaged peak-current responses to select compounds from cells expressing α9 alone (taken from Figures 2 & 4) or α9 co-expressed with α10. The only significant difference was in the responses to p-Br ($p < 0.05$ after correction for multiple comparisons). **C)** Concentration-response relationships for p-CF3 for the activation of cells (n = 6) co-expressing α9 with α10, for comparison to the data in Figure 5. **D)** Concentration-response relationships of select compounds for the inhibition of the ACh responses of cells co-expressing α9 with α10, for comparison to the data in Figure 6.

α9 agonists and antagonists

Selectivity of α9 agonists

We evaluated the α9 agonists *p*-CONH, p-CN, PhDu, and CF_3PhDu and the α9 antagonists *o*-Cl, *p*-Fl, *m*-CF_3, *p*-MeO, diMeO, 2-nap, and *m*-CONH for their ability to activate or inhibit other nAChR subtypes. Agonist activity was evaluated by applying the compounds at 100 μM to high sensitivity α4β2 receptors with the subunit stoichiometry α4(2)β2(3) [34], low sensitivity α4β2 (α4(3)β2(2)) receptors, α3β4 receptors, and cells expressing the mouse muscle α1β1εδ subunits. In no case did the compounds evoke a response as large as 3% the respective ACh controls (10 μM, 100 μM, 100 μM, and 30 μM for α4(2)β2(3), α4(2)β2(3), α3β4, and α1β1εδ, respectively), basically at our limit of detection (data not shown). To evaluate inhibitory activity on the same receptor subtypes, as well as for α7, control concentrations of ACh (60 μM, 10 μM, 100 μM, 100 μM, and 30 μM for α7, α4(2)β2(3), α4(2)β2(3), α3β4, and α1β1εδ, respectively) were co-applied with 3 μM of the test compounds, 3 μM being a concentration in the range of the potency for α9 activity. The inhibitory activity was generally low (Table 4).

Table 4

Receptor inhibition.

Responses to ACh co-applied with 3μM test compound compared to ACh alone

Compound	LSα4(3)β2(2)	HS α4(2)β2(3)	α3β4	α1β1εδ	α7
p-CONH	0.995 ± 0.020	0.813 ± 0.020	0.887 ± 0.021	0.692 ± 0.069	0.993 ± 0.041
p-CN	0.964 ± 0.045	0.815 ± 0.020	1.104 ± 0.071	0.687 ± 0.047	0.870 ± 0.015
PhDu	0.940 ± 0.040	0.692 ± 0.033	0.837 ± 0.023	0.642 ± 0.057	0.755 ± 0.011
CF_3PhDu	0.819 ± 0.078	0.671 ± 0.015	0.704 ± 0.031	0.427 ± 0.033	0.679 ± 0.026
o-Cl	0.876 ± 0.048	0.964 ± 0.013	0.614 ± 0.033	0.452 ± 0.024	1.048 ± 0.172
p-Fl	0.928 ± 0.041	0.811 ± 0.039	0.827 ± 0.034	0.618 ± 0.030	0.768 ± 0.008
m-CF_3	0.876 ± 0.050	0.810 ± 0.019	0.514 ± 0.045	0.517 ± 0.082	0.673 ± 0.035
p-MeO	0.895 ± 0.066	0.958 ± 0.023	0.767 ± 0.040	0.894 ± 0.032	0.866 ± 0.018
diMeO	0.970 ± 0.027	1.108 ± 0.026	0.698 ± 0.049	0.851 ± 0.050	0.839 ± 0.009
2-Nap	0.504 ± 0.109	0.507 ± 0.029	0.279 ± 0.043	0.692 ± 0.049	0.651 ± 0.027
m-CONH	0.854 ± 0.051	0.865 ± 0.048	0.547 ± 0.050	0.920 ± 0.029	0.722 ± 0.023

*Data on α7 are based on based on reduction of net charge. Data for heteromeric receptors are based on reduction of peak currents.

Structure basis for α9 agonism

Though an experimental high resolution three-dimensional structure for the α9 nAChR does not yet exist, we wished to place the experimental results described here in a structural context. We therefor used the reported experimental EM structure for the homologous α7 receptor with bound agonist [35] as a template for construction of a homology model for the α9 receptor. Two caveats bear mention here. First a homology model provides a good guess to the overall protein fold with less certainty about side chain and subunit interface configurations. Secondly, docking programs will allow one to establish how a compound might fit into a binding site, and ranks the different binding poses via empirical scoring functions. With these considerations in mind, we used the α9 receptor homology model to dock in a series agonists and antagonists to discern possible differences in binding within the group. The results presented

α9 agonists and antagonists

in Figure 8A allowed us to identify two unique binding pocket subsites; one associated with antagonists and the other with agonists.

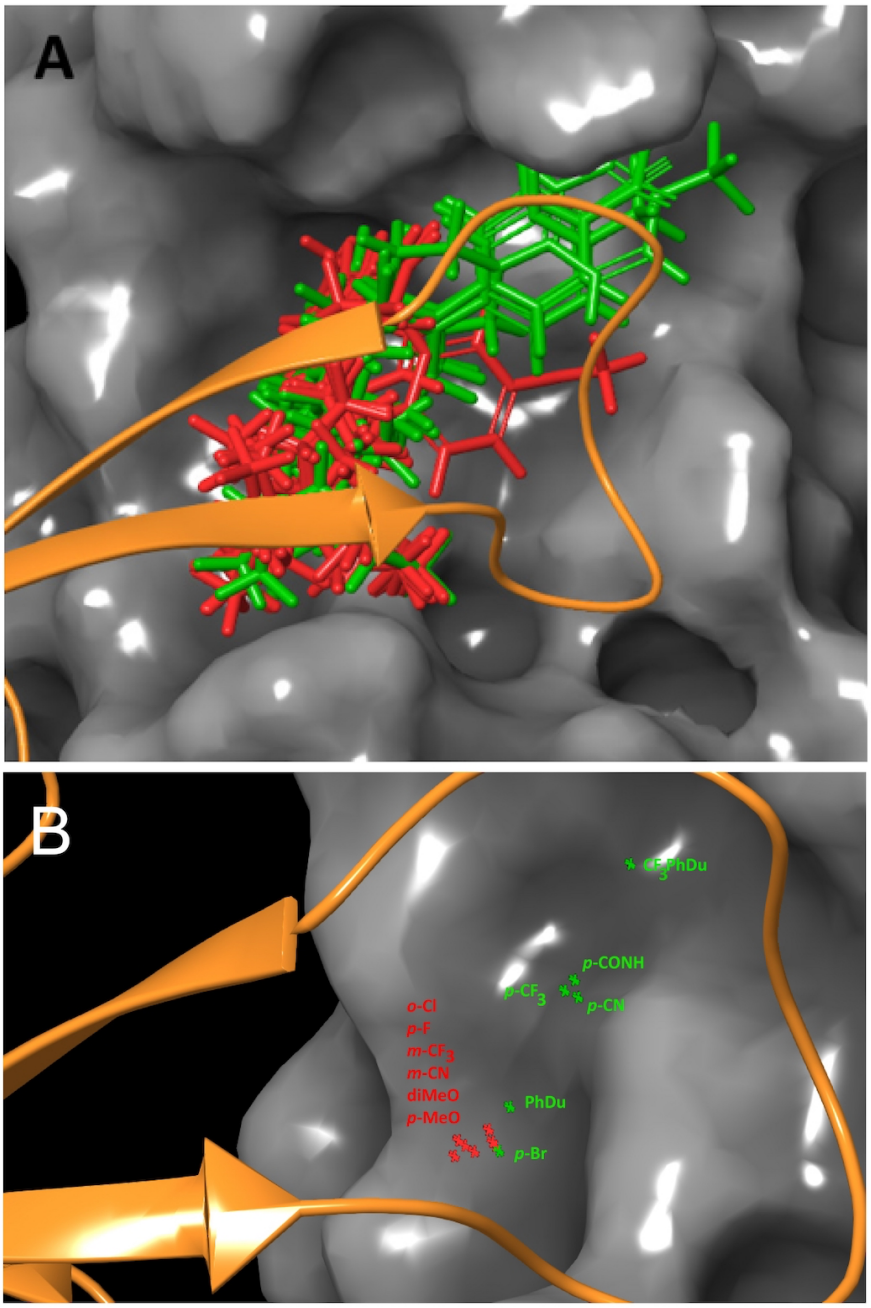

Figure 8. Two binding pockets for antagonists and agonists in α9. A) A total of 12 agonists and antagonists of a9 were docked into the α9 homology model. Agonists are colored green, antagonists are colored in red. The (+) face C-loop is shown is orange, and the (-) face of the interface is shown as a surface in gray. Agonists place the aryl ring in an extended binding groove on the (-) face, towards the upper right of the image, whereas antagonists place the aryl ring in a smaller internal pocket within the interface. Some of the ribbon for the (+) chain was omitted for clarity. The following compounds were docked: *p*-CF_3, *p*-Br, *p*-CONH, *p*-CN, PhDu, CF_3PhDu, *o*-Cl, *p*-F, *m*-CF_3, *m*-CN, DiMeO, and *p*-MeO. **B)** Agonists and antagonists tend to place their charged ammonium group in different locations under the C-loop. Using the poses shown in panel A, all but the positions of the ammonium group were hidden from view. Green stars indicate the position of agonist ammonium groups, while red stars indicate the position of antagonists. Notable outliers from the trend are the very weak agonist *p*-Br, which groups with antagonists, and PhDu, a full agonist that groups with antagonists.

α9 agonists and antagonists

The sites were primarily composed of residues on the (-) side of the interface, and recognized the aryl group on the piperazine ring. Key residues for the antagonist site were the side chains of V108 and T116. Critical residues for the agonist subsite included residues C192 and S193 of the C-loop and T116 and R110 of the (-) face. We observed a second trend in the docking data, namely that the location of the ammonium center of the piperazine ring strongly tended to group differently for antagonists versus agonists. This is presented in Figure 8B. We note that compound PhDu, an agonist, grouped with the antagonists in regard to the location of its ammonium group. Interestingly, the very weak agonist *p*-Br also grouped with the antagonists. It is fascinating that the antagonists actually did a better job of fitting their positive charge into the canonical cation-π box under the C-loop, compared to the position the agonists did.

Evaluation of a novel compound on the diEPP scaffold

Based on the predictions from the models, a new compound, 1,1-diethyl-4-(4-((6-methylpyridin-2-yl)carbamoyl)phenyl)piperazin-1-ium iodide (APA-diEPP) was synthesized. The compound evoked relatively small responses from cells expressing α7 (Figure 9) (I_{Max} 0.42 ± 0.03 compared to ACh, with an EC_{50} = 6.4 ± 1.7 μM) and appeared to be a potent full agonist for α9 (I_{Max} 1.11 ± 0.03 compared to ACh, with an EC_{50} = 0.67 ± 0.08 μM).

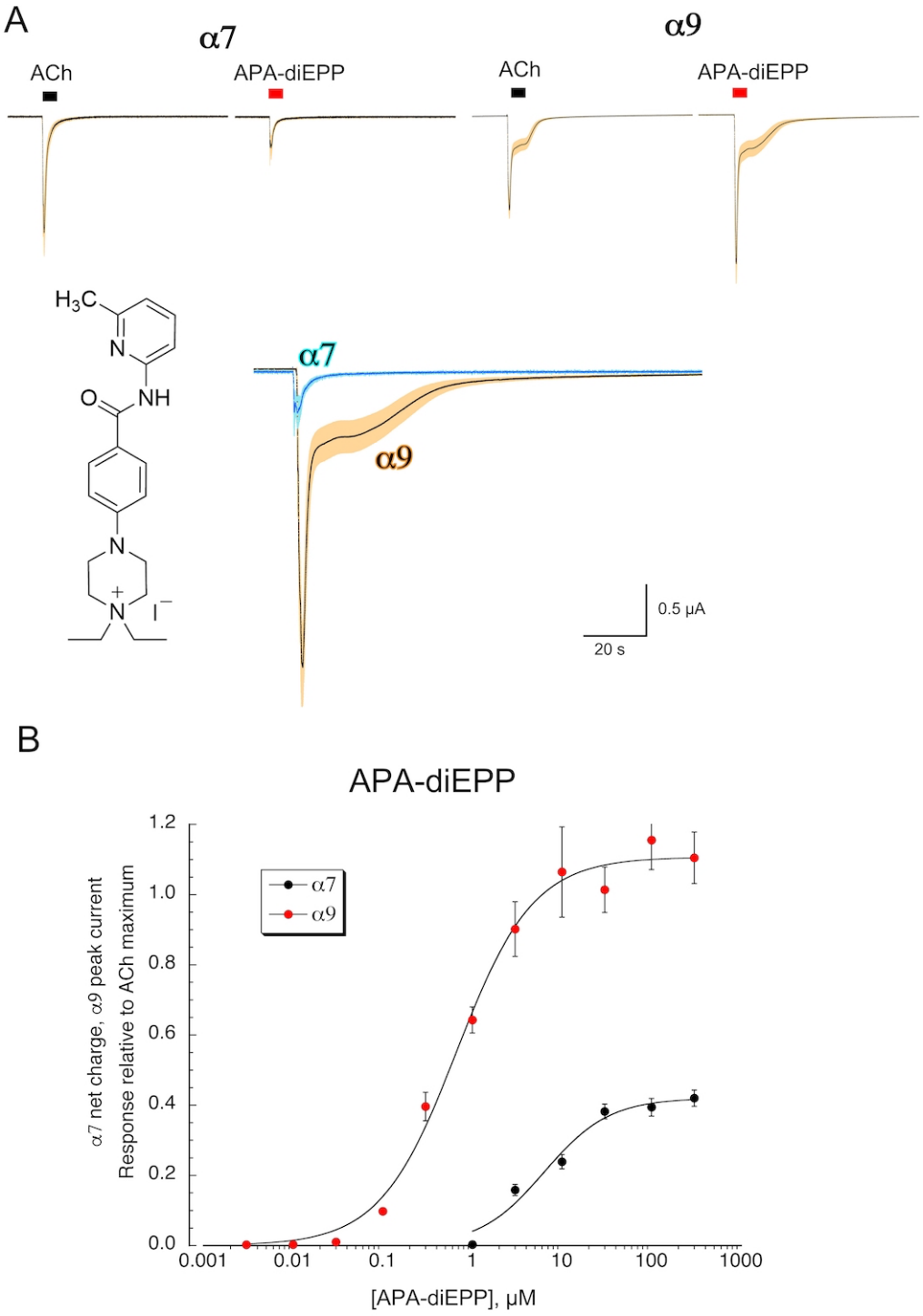

Figure 9. Characterization of APA-diEPP. **A)** Averaged raw data traces for 100 μM APA-diEPP applications on cells expressing α7 (left, n = 7) or α9 (right, n = 6) and their respective 60 μM ACh controls. The average normalized responses are shown below along with the structure of APA-diEPP. **B)** Concentration-response relationships of APA-diEPP for the activation of cells expressing α7 (net charge, n = 7) or α9 (peak currents, n = 6). Experiment responses were measured relative to the preceding ACh control responses and then normalized relative to the ratio of the ACh controls to the ACh maximum.

Summary

The α9α10 nAChR of the inner ear were not only the last nAChR to be cloned, but they have remained, until now, some of the most difficult nicotinic receptors to target pharmacologically. They are sensitive to α-BTX, but that is a feature they share with α7 and muscle-type receptors. The only α9-selective antagonists identified prior to this study have been conotoxins such as RgIA4 [26], and peptide toxins are difficult to synthesize and purify, and generally impractical as therapeutic agents, due to stability and bioavailability issues [36]. Likewise, previously there have been no reports of α9α10-selective agonists, and several common nAChR agonists such as nicotine, cytisine, and epibatidine are, in fact, antagonists of these receptors [6]. Our results therefore represent several new opportunities for investigating the function of α9α10 nAChR, as well as potential new directions for development of therapeutics.

Translational potential

One potential direction for therapeutic development is in regard to hearing disorders [37]. The cholinergic efferent fibers innervating outer hair cells can serve to protect the inner ear from damage resulting from acute or chronic presentation of loud noise that can cause noise-induced hearing loss, a common workplace hazard [38]. Agonists for α9α10 receptors could enhance the effectiveness of this system [37] and be protective [39]. Agonists for α9α10 might also prove useful an as adjuvant in auditory training of dyslexic children [37, 40]. Tinnitus (ringing in the ears) is a condition that approximately one in ten people suffer at least sporadically and perhaps as many as one in 100 people experience chronically [41]. It has been proposed that an α9α10 antagonist, probably in conjunction with a central nervous system agent, could be used to treat this condition [37].

The other important area for potential therapeutic development is the management of neuropathic and inflammatory pain [42-43], a direction supported by numerous studies with the α9α10-selective conotoxins [28-29, 44-47]. While these conotoxin studies point to the inhibition of α9α10 receptors as the therapeutic modality, an alternative perspective from work with phosphocholine [30, 48] suggests that atypical agonism of α9 receptors may be the basis for the anti-inflammatory effects of α9 drugs. It has previously been demonstrated that p-CF_3, a compound we have identified as a partial agonist for both α7 and α9, was effective at reducing inflammatory and neuropathic pain in an animal model [31].

In light of the current epidemic in opioid use [49], research in the area of alternative pain therapies is extremely important. The role of α7 in the modulation of CAP is well established [19, 50-51], but, as noted above, the exact role of α9α10 receptors is less clear.

Future directions

In the present study, we identify a range of activities in our test compounds, on both α7 and α9 receptors, without any real correlation in the two types of activity. Amongst our most efficacious α7 partial agonists (Figure 2), we identified both a potent α9 antagonist (*o*-Cl) and an excellent α9 agonist (*p*-CN). This range of activities and the potential separation of α7 and α9 effects may be instrumental in

determining the optimal profile for future development of optimized therapeutics. The results derived from our modeling and docking with the α9 receptor indicated that the aryl ring of N-aryl piperazines found a surface accessible unique binding subsite associated with agonists, whereas antagonists placed the aryl ring in a smaller internal subsite pocket. As an initial test of the utility of the model we hypothesized that larger substituents on the aryl ring would maintain and perhaps enhance selectivity for α9 agonism over α7 activity, and this proved to be the case with APA-diEPP which we synthesized and found had a nearly 10-fold higher potency for α9, and was a full agonist for this receptor while only a partial agonist for α7. The insights provided by our α9 model has aided in generating a roadmap for the design of such new α9 selective drugs.

Methods and materials

Chemicals and reagents

Acetylcholine chloride (ACh) and buffer chemicals were purchased from Sigma-Aldrich Chemical Company (St. Louis, MO). PNU-120596 was synthesized in the Horenstein laboratory by Dr. Kinga Chojnacka following the published procedure [52]. The 1,1-diethyl-4-phenylpiperazin-1-ium derivatives were synthesized as previously documented [32]. The synthesis of 1-ethyl-4-phenylthiomorpholin-1-ium (EPTMO) was as previously described [33]. The experimental compounds were dissolved in DMSO at 100mM and diluted to test concentrations in Ringer's solution freshly just before use. Stock solutions were held -20º.

The synthesis and chemical characterization of the three compounds not previously published; 3-phenyl-3,6-diazaspiro[5.5]undecan-6-ium (PhDu), 3-(4-(trifluoromethyl)phenyl)-3,6-diazaspiro[5.5]undecan-6-ium (CF_3PhDu), and 1,1-diethyl-4-(4-((6-methylpyridin-2-yl)carbamoyl)phenyl)piperazin-1-ium iodide (APA-diEPP) are described in the supplemental data. Compounds were tested as their iodide salts.

Molecular docking into the α9 nAChR orthosteric site.

A homology model for α9 was created using the SwissModel server [53] with the recently revised EM structure 7KOQ for the α7 nAChR as template. The model, in dimeric form was used for docking studies using Glide in XP mode (Schrodinger, Inc) [54]. The grid employed was sufficiently large as to encompass the orthosteric site of the receptor. Poses presented for docked compounds represent those with the top Glide score for each.

Expression of human nAChR subunits in Xenopus laevis *oocytes*

Plasmid DNAs encoding the human α7 and heteromeric nAChR were obtained from Jon Lindstrom (University of Pennsylvania, Philadelphia, PA). Mouse muscle subunit clones were obtained from Jim Boulter (Salk Institute, La Jolla CA) and Paul Gardner (Dartmouth, Hanover NH). The human resistance-to-cholinesterase 3 (RIC3) clone was obtained from Millet Treinin (Hebrew University, Jerusalem, Israel) and RNA co-injected with α7 to improve the level and speed of receptor expression

without affecting their pharmacological properties [55]. Plasmid DNA encoding the human α10 nAChR was obtained from J. Michael McIntosh. Plasmid DNA encoding the human α9 nAChR and the human receptor-associated protein of the synapse (RAPSYN) with codon optimization for expression in *Xenopus laevis* were obtained from Katrin Richter. RAPSYN RNA was co-injected with the α9 and α10 to improve expression [30]. After linearization and purification of the plasmid DNAs, RNAs were prepared using the mMessage mMachine in vitro RNA transcription kit (Ambion, Austin, TX).

Frogs were maintained in the Animal Care Service facility of the University of Florida, and all procedures were approved by the University of Florida Institutional Animal Care and Use Committee (approval number 202002669). In brief, the animals were first anesthetized for 15-20 min in 1.5 l frog tank water containing 1 g of MS-222 buffered with sodium bicarbonate. Oocytes were obtained surgically from mature female *Xenopus laevis* (Nasco, Ft. Atkinson, WI) and treated with 1.4 mg/ml type 1 collagenase (Worthington Biochemicals, Freehold, NJ, USA) for 2-4 h at room temperature in calcium-free Barth's solution (88 mM NaCl, 1 mM KCl, 2.38 mM $NaHCO_3$, 0.82 mM $MgSO_4$, 15 mM HEPES, and 12 mg/l tetracycline, pH 7.6) to remove the ovarian tissue and the follicular layers. Stage V oocytes were injected with 4-6 ng α7 RNA and 2-3 ng RIC3 RNA (2:1 ratio) in 50 nl water, or with 12 ng α9 RNA, or along with 12 ng α10 RNA, and 3 ng RAPSYN RNA in 50 nl water. Oocytes were maintained in Barth's solution containing additionally 0.32 mM $Ca(NO_3)_2$ and 0.41 mM $CaCl_2$, and recordings were carried out 2-20 days after injection.

Two-electrode voltage-clamp electrophysiology

Two-electrode voltage-clamp experiments were conducted using OpusXpress 6000A (Molecular Devices, Union City, CA, USA) [56]. Both the voltage and current electrodes were filled with 3 M KCl. Oocytes were voltage-clamped at -60 mV at RT. The oocytes were perfused with Ringer's solution (115 mM NaCl, 2.5 mM KCl, 1.8 mM $CaCl_2$, 10 mM HEPES, pH 7.2) at 2 ml/min for α7, α9, and α9α10 experiments, or at 4 ml/min for heteromeric receptor experiments. To evaluate the effects of experimental compounds, responses were compared to control ACh-evoked responses, defined as the average of two initial applications of 60 μM ACh made before test applications. Drug applications were 12 s for α7, α9, and α9α10 or 6 s for heteromeric receptors in duration followed by 181 s washout periods for α7, α9, and α9α10 or 241 s for heteromeric receptors.

The responses were calculated as both peak-current amplitudes and net charge, as previously described [57]. Data were collected at 50 Hz, filtered at 20 Hz, and analyzed by Clampfit (Molecular Devices) and Excel (Microsoft, Redmond, WA, USA). Data were expressed as means ± SEM from at least four oocytes for each experiment and plotted with Kaleidagraph 4.5.2 (Abelbeck Software, Reading, PA, USA). Each episode of data acquisition was a total of 210 s and included an initial 30 s period used to define the baseline for the drug-evoked responses. After 30 s, drugs were applied, and the following 120 s were defined as the drug response period for analysis. Data reported for α7 were net charge, while peak currents are used for α9* responses since these receptors do not show the same concentration-dependent desensitization that invalidates peak currents as measurements of α7 concentration-dependent

responses [57]. Multi-cell averages were calculated for comparisons of complex responses. Averages of the normalized data were calculated for each of the 10,322 points in each of the 206.44 s traces (acquired at 50 Hz), as well as the standard errors for those averages.

Statistical analyses and data processing.

In two-electrode voltage-clamp experiments, the comparisons of results were made using one-way ANOVA or using t-tests between the pairs of experimental measurements. In cases where multiple comparisons were made, a Bonferroni correction for multiple comparisons [58] was applied to correct for possible false positives. A value of $p \leq 0.05$ was used to constitute a minimum level of significance. The statistics were calculated using an Excel template provided in Microsoft Office or ANOVA protocols in Kaleidagraph (4.5.2 Abelbeck Software, Reading, PA). Concentration-response relationships utilized data obtained over a range of concentration at roughly half log units. The Levenberg-Marquardt algorithm was used in Kaleidagraph to generate curves based on the Hill equation that best fit the data.

This work was supported by NIH grant, GM57481

Authorship Contributions

Participated in research design: NAH, HA, CS, RLP,
Conducted experiments: CS, MQ
Contributed new reagents or analytic tools: MQ, HA
Performed data analysis: CS, NAH, HA, RLP
Wrote or contributed to the writing of the manuscript: NAH, RLP

Supporting Information: Synthetic procedures, ^{1}H- and ^{13}C-NMR, and MS data for new compounds.

Acknowledgements: We are especially grateful to Katrin Richter and Veronika Grau for sharing the codon optimized α9 and rapsyn clones. Oocyte recordings were done by Wenchi Corrie Lu.

The authors report they have no conflicts of interest.

References

1. Papke, R. L., Merging old and new perspectives on nicotinic acetylcholine receptors. *Biochem Pharmacol* **2014,** *89* (1), 1-11.
2. Rasmussen, G. L., Further observations of the efferent cochlear bundle. *J Comp Neurol* **1953,** *99* (1), 61-74.
3. Fex, J., Auditory activity in centrifugal and centripetal cochlear fibres in cat. A study of a feedback system. *Acta Physiol Scand Suppl* **1962,** *189*, 1-68.
4. Fex, J.; Adams, J. C., alpha-Bungarotoxin blocks reversibly cholinergic inhibition in the cochlea. *Brain Res* **1978,** *159* (2), 440-4.
5. Elgoyhen, A. B.; Johnson, D. S.; Boulter, J.; Vetter, D. E.; Heinemann, S., a9: An acetylcholine receptor with novel pharmacological properties expressed in rat cochlear hair cells. *Cell* **1994,** *79*, 705-715.
6. Verbitsky, M.; Rothlin, C. V.; Katz, E.; Elgoyhen, A. B., Mixed nicotinic-muscarinic properties of the alpha9 nicotinic cholinergic receptor. *Neuropharmacology* **2000,** *39* (13), 2515-24.
7. Vetter, D. E.; Liberman, M. C.; Mann, J.; Barhanin, J.; Boulter, J.; Brown, M. C.; Saffiote-Kolman, J.; Heinemann, S. F.; Elgoyhen, A. B., Role of alpha9 nicotinic ACh receptor subunits in the development and function of cochlear efferent innervation. *Neuron* **1999,** *23* (1), 93-103.
8. Boulter, J.; Elgoyhen, B.; Katz, E.; Rothlin, C.; Vetter, D., Alpha 10: A novel nicotinic acetylcholine receptor subunit gene. *Unpublished* **1999,** *GenBank accession number*, AF196344.
9. Elgoyhen, A. B.; Vetter, D. E.; Katz, E.; Rothlin, C. V.; Heinemann, S. F.; Boulter, J., alpha10: a determinant of nicotinic cholinergic receptor function in mammalian vestibular and cochlear mechanosensory hair cells. *Proc Natl Acad Sci U S A* **2001,** *98* (6), 3501-6.
10. Plazas, P. V.; Katz, E.; Gomez-Casati, M. E.; Bouzat, C.; Elgoyhen, A. B., Stoichiometry of the alpha9alpha10 nicotinic cholinergic receptor. *J Neurosci* **2005,** *25* (47), 10905-12.
11. Katz, E.; Elgoyhen, A. B.; Gomez-Casati, M. E.; Knipper, M.; Vetter, D. E.; Fuchs, P. A.; Glowatzki, E., Developmental regulation of nicotinic synapses on cochlear inner hair cells. *J Neurosci* **2004,** *24* (36), 7814-20.
12. Lykhmus, O.; Voytenko, L. P.; Lips, K. S.; Bergen, I.; Krasteva-Christ, G.; Vetter, D. E.; Kummer, W.; Skok, M., Nicotinic Acetylcholine Receptor alpha9 and alpha10 Subunits Are Expressed in the Brain of Mice. *Front Cell Neurosci* **2017,** *11*, 282.
13. Morley, B. J.; Whiteaker, P.; Elgoyhen, A. B., Commentary: Nicotinic Acetylcholine Receptor alpha9 and alpha10 Subunits Are Expressed in the Brain of Mice. *Front Cell Neurosci* **2018,** *12*, 104.
14. Lips, K. S.; Pfeil, U.; Kummer, W., Coexpression of alpha 9 and alpha 10 nicotinic acetylcholine receptors in rat dorsal root ganglion neurons. *Neuroscience* **2002,** *115* (1), 1-5.
15. Callaghan, B.; Adams, D. J., Analgesic alpha-conotoxins Vc1.1 and RgIA inhibit N-type calcium channels in sensory neurons of alpha9 nicotinic receptor knockout mice. *Channels (Austin)* **2010,** *4* (1), 51-4.
16. Chaicumpa, W.; Ybanez, L.; Kitikoon, V.; Pungpak, S.; Ruangkunaporn, Y.; Chongsa-nguan, M.; Sornmani, S., Detection of Opisthorchis viverrini antigens in stools using specific monoclonal antibody. *Int J Parasitol* **1992,** *22* (4), 527-31.
17. Biallas, S.; Wilker, S.; Lips, K. S.; Kummer, W.; Grando, S. A.; Padberg, W.; Grau, V., Immunohistochemical detection of nicotinic acetylcholine receptor subunits alpha9 and alpha10 in rat lung isografts and allografts. *Life Sci* **2007,** *80* (24-25), 2286-9.
18. Peng, H.; Ferris, R. L.; Matthews, T.; Hiel, H.; Lopez-Albaitero, A.; Lustig, L. R., Characterization of the human nicotinic acetylcholine receptor subunit alpha (alpha) 9 (CHRNA9) and alpha (alpha) 10 (CHRNA10) in lymphocytes. *Life Sci* **2004,** *76* (3), 263-80.
19. Rosas-Ballina, M.; Tracey, K. J., Cholinergic control of inflammation. *J Intern Med* **2009,** *265* (6), 663-79.

20. Tracey, K. J., Physiology and immunology of the cholinergic antiinflammatory pathway. *The Journal of clinical investigation* **2007,** *117* (2), 289-96.
21. Rosas-Ballina, M.; Goldstein, R. S.; Gallowitsch-Puerta, M.; Yang, L.; Valdes-Ferrer, S. I.; Patel, N. B.; Chavan, S.; Al-Abed, Y.; Yang, H.; Tracey, K. J., The selective alpha7 agonist GTS-21 attenuates cytokine production in human whole blood and human monocytes activated by ligands for TLR2, TLR3, TLR4, TLR9, and RAGE. *Mol Med* **2009,** *15* (7-8), 195-202.
22. Horenstein, N. A.; Papke, R. L., Anti-inflammatory Silent Agonists. *ACS Med Chem Lett* **2017,** *8* (10), 989-991.
23. Bagdas, D. A.; Wilkerson, J. L.; Kulkarni, A.; Toma, W.; AlSharari, S.; Gul, Z.; Lichtman, A. H.; Papke, R. L.; Thakur, G. A.; Damaj, M. I., The alpha7 nicotinic receptor dual allosteric agonist and positive allosteric modulator GAT107 reverses nociception in mouse models of inflammatory and neuropathic pain. *Br. J. Pharm* **2016,** *173* (16), 2506-20.
24. Kabbani, N.; Nichols, R. A., Beyond the Channel: Metabotropic Signaling by Nicotinic Receptors. *Trends Pharmacol Sci* **2018,** *39* (4), 354-366.
25. Whiteaker, P.; Marks, M. J.; Christensen, S.; Dowell, C.; Collins, A. C.; McIntosh, J. M., Synthesis and characterization of 125I-alpha-conotoxin ArIB[V11L;V16A], a selective alpha7 nicotinic acetylcholine receptor antagonist. *J Pharmacol Exp Ther* **2008,** *325* (3), 910-9.
26. Azam, L.; McIntosh, J. M., Molecular basis for the differential sensitivity of rat and human alpha9alpha10 nAChRs to alpha-conotoxin RgIA. *J Neurochem* **2012,** *122* (6), 1137-44.
27. Bagdas, D.; Gurun, M. S.; Flood, P.; Papke, R. L.; Damaj, M. I., New Insights on Neuronal Nicotinic Acetylcholine Receptors as Targets for Pain and Inflammation: A Focus on alpha7 nAChRs. *Curr Neuropharmacol* **2018,** *16* (4), 415-425.
28. Christensen, S. B.; Hone, A. J.; Roux, I.; Kniazeff, J.; Pin, J. P.; Upert, G.; Servent, D.; Glowatzki, E.; McIntosh, J. M., RgIA4 Potently Blocks Mouse alpha9alpha10 nAChRs and Provides Long Lasting Protection against Oxaliplatin-Induced Cold Allodynia. *Front Cell Neurosci* **2017,** *11*, 219.
29. AlSharari, S. D.; Toma, W.; Mahmood, H. M.; Michael McIntosh, J.; Imad Damaj, M., The alpha9alpha10 nicotinic acetylcholine receptors antagonist alpha-conotoxin RgIA reverses colitis signs in murine dextran sodium sulfate model. *Eur J Pharmacol* **2020,** *883*, 173320.
30. Richter, K.; Mathes, V.; Fronius, M.; Althaus, M.; Hecker, A.; Krasteva-Christ, G.; Padberg, W.; Hone, A. J.; McIntosh, J. M.; Zakrzewicz, A.; Grau, V., Phosphocholine - an agonist of metabotropic but not of ionotropic functions of alpha9-containing nicotinic acetylcholine receptors. *Sci Rep* **2016,** *6*, 28660.
31. Quadri, M.; Bagdas, D.; Toma, W.; Stokes, C.; Horenstein, N. A.; Damaj, M. I.; Papke, R. L., The antinociceptive and anti-inflammatory properties of the alpha7 nAChR weak partial agonist p-CF3N,N-diethyl-N'-phenylpiperazine. *J Pharmacol Exp Ther* **2018,** *367* (2), 203-214.
32. Quadri, M.; Papke, R. L.; Horenstein, N. A., Dissection of N,N-diethyl-N'-phenylpiperazines as alpha7 nicotinic receptor silent agonists. *Bioorganic & medicinal chemistry* **2016,** *24* (2), 286-93.
33. Quadri, M.; Stokes, C.; Gulsevin, A.; Felts, A. C. J.; Abboud, K. A.; Papke, R. L.; Horenstein, N. A., Sulfonium as a Surrogate for Ammonium: A New alpha7 Nicotinic Acetylcholine Receptor Partial Agonist with Desensitizing Activity. *J Med Chem* **2017,** *60* (18), 7928-7934.
34. Zhou, Y.; Nelson, M. E.; Kuryatov, A.; Choi, C.; Cooper, J.; Lindstrom, J., Human alpha4beta2 acetylcholine receptors formed from linked subunits. *J Neurosci* **2003,** *23* (27), 9004-15.
35. Noviello, C. M.; Gharpure, A.; Mukhtasimova, N.; Cabuco, R.; Baxter, L.; Borek, D.; Sine, S. M.; Hibbs, R. E., Structure and gating mechanism of the alpha7 nicotinic acetylcholine receptor. *Cell* **2021**.
36. Giribaldi, J.; Haufe, Y.; Evans, E. R. J.; Amar, M.; Durner, A.; Schmidt, C.; Faucherre, A.; Moha Ou Maati, H.; Enjalbal, C.; Molgo, J.; Servent, D.; Wilson, D. T.; Daly, N. L.; Nicke, A.; Dutertre, S.,

Backbone Cyclization Turns a Venom Peptide into a Stable and Equipotent Ligand at Both Muscle and Neuronal Nicotinic Receptors. *J Med Chem* **2020,** *63* (21), 12682-12692.
37. Elgoyhen, A. B.; Katz, E.; Fuchs, P. A., The nicotinic receptor of cochlear hair cells: a possible pharmacotherapeutic target? *Biochem Pharmacol* **2009,** *78* (7), 712-9.
38. Davis, R., Long-term noise exposures: A brief review. *Hear Res* **2017,** *349*, 31-33.
39. Reiter, E. R.; Liberman, M. C., Efferent-mediated protection from acoustic overexposure: relation to slow effects of olivocochlear stimulation. *J Neurophysiol* **1995,** *73* (2), 506-14.
40. Kumar, U. A.; Vanaja, C. S., Functioning of olivocochlear bundle and speech perception in noise. *Ear Hear* **2004,** *25* (2), 142-6.
41. Moller, A. R., Tinnitus: presence and future. *Prog Brain Res* **2007,** *166*, 3-16.
42. Toma, W.; Ulker, E.; Alqasem, M.; AlSharari, S. D.; McIntosh, J. M.; Damaj, M. I., Behavioral and Molecular Basis of Cholinergic Modulation of Pain: Focus on Nicotinic Acetylcholine Receptors. *Curr Top Behav Neurosci* **2020,** *45*, 153-166.
43. Hone, A. J.; Servent, D.; McIntosh, J. M., alpha9-containing nicotinic acetylcholine receptors and the modulation of pain. *Br J Pharmacol* **2018,** *175* (11), 1915-1927.
44. Huynh, P. N.; Giuvelis, D.; Christensen, S.; Tucker, K. L.; McIntosh, J. M., RgIA4 Accelerates Recovery from Paclitaxel-Induced Neuropathic Pain in Rats. *Mar Drugs* **2019,** *18* (1).
45. Romero, H. K.; Christensen, S. B.; Di Cesare Mannelli, L.; Gajewiak, J.; Ramachandra, R.; Elmslie, K. S.; Vetter, D. E.; Ghelardini, C.; Iadonato, S. P.; Mercado, J. L.; Olivera, B. M.; McIntosh, J. M., Inhibition of alpha9alpha10 nicotinic acetylcholine receptors prevents chemotherapy-induced neuropathic pain. *Proc Natl Acad Sci U S A* **2017,** *114* (10), E1825-E1832.
46. Pacini, A.; Micheli, L.; Maresca, M.; Branca, J. J.; McIntosh, J. M.; Ghelardini, C.; Di Cesare Mannelli, L., The alpha9alpha10 nicotinic receptor antagonist alpha-conotoxin RgIA prevents neuropathic pain induced by oxaliplatin treatment. *Exp Neurol* **2016,** *282*, 37-48.
47. Di Cesare Mannelli, L.; Cinci, L.; Micheli, L.; Zanardelli, M.; Pacini, A.; McIntosh, J. M.; Ghelardini, C., alpha-conotoxin RgIA protects against the development of nerve injury-induced chronic pain and prevents both neuronal and glial derangement. *Pain* **2014,** *155* (10), 1986-95.
48. Zakrzewicz, A.; Richter, K.; Agne, A.; Wilker, S.; Siebers, K.; Fink, B.; Krasteva-Christ, G.; Althaus, M.; Padberg, W.; Hone, A. J.; McIntosh, J. M.; Grau, V., Canonical and Novel Non-Canonical Cholinergic Agonists Inhibit ATP-Induced Release of Monocytic Interleukin-1beta via Different Combinations of Nicotinic Acetylcholine Receptor Subunits alpha7, alpha9 and alpha10. *Front Cell Neurosci* **2017,** *11*, 189.
49. Ayoo, K.; Mikhaeil, J.; Huang, A.; Wasowicz, M., The opioid crisis in North America: facts and future lessons for Europe. *Anaesthesiol Intensive Ther* **2020,** *52* (2), 139-147.
50. Sitapara, R. A.; Gauthier, A. G.; Valdes-Ferrer, S. I.; Lin, M.; Patel, V.; Wang, M.; Martino, A. T.; Perron, J. C.; Ashby, C. R., Jr.; Tracey, K. J.; Pavlov, V. A.; Mantell, L. L., The alpha7 nicotinic acetylcholine receptor agonist, GTS-21, attenuates hyperoxia-induced acute inflammatory lung injury by alleviating the accumulation of HMGB1 in the airways and the circulation. *Mol Med* **2020,** *26* (1), 63.
51. Wang, H.; Yu, M.; Ochani, M.; Amella, C. A.; Tanovic, M.; Susarla, S.; Li, J. H.; Yang, H.; Ulloa, L.; Al-Abed, Y.; Czura, C. J.; Tracey, K. J., Nicotinic acetylcholine receptor alpha7 subunit is an essential regulator of inflammation. *Nature* **2003,** *421* (6921), 384-8.
52. Hurst, R. S.; Hajos, M.; Raggenbass, M.; Wall, T. M.; Higdon, N. R.; Lawson, J. A.; Rutherford-Root, K. L.; Berkenpas, M. B.; Hoffmann, W. E.; Piotrowski, D. W.; Groppi, V. E.; Allaman, G.; Ogier, R.; Bertrand, S.; Bertrand, D.; Arneric, S. P., A novel positive allosteric modulator of the alpha7 neuronal nicotinic acetylcholine receptor: in vitro and in vivo characterization. *J Neurosci* **2005,** *25* (17), 4396-405.
53. Biasini, M.; Bienert, S.; Waterhouse, A.; Arnold, K.; Studer, G.; Schmidt, T.; Kiefer, F.; Cassarino, T. G.; Bertoni, M.; Bordoli, L.; Schwede, T., SWISS-MODEL: modelling protein tertiary and

quaternary structure using evolutionary information. *Nucleic Acids Res* **2014,** *42* (Web Server issue), W252-8.
54. Dixon, S. L.; Smondyrev, A. M.; Knoll, E. H.; Rao, S. N.; Shaw, D. E.; Friesner, R. A., PHASE: a new engine for pharmacophore perception, 3D QSAR model development, and 3D database screening: 1. Methodology and preliminary results. *Journal of computer-aided molecular design* **2006,** *20* (10-11), 647-71.
55. Halevi, S.; Yassin, L.; Eshel, M.; Sala, F.; Sala, S.; Criado, M.; Treinin, M., Conservation within the RIC-3 gene family. Effectors of mammalian nicotinic acetylcholine receptor expression. *J Biol Chem* **2003,** *278* (36), 34411-7.
56. Papke, R. L.; Stokes, C., Working with OpusXpress: methods for high volume oocyte experiments. *Methods* **2010,** *51* (1), 121-33.
57. Papke, R. L.; Papke, J. K. P., Comparative pharmacology of rat and human alpha7 nAChR conducted with net charge analysis. *Br J of Pharm* **2002,** *137* (1), 49-61.
58. Aickin, M.; Gensler, H., Adjusting for multiple testing when reporting research results: the Bonferroni vs Holm methods. *American journal of public health* **1996,** *86* (5), 726-8.